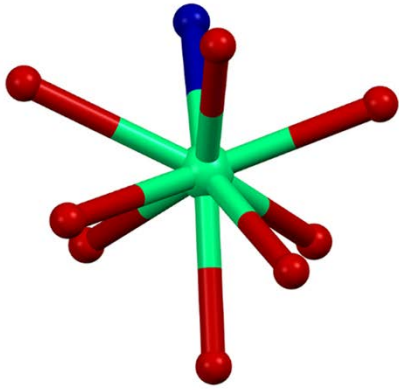
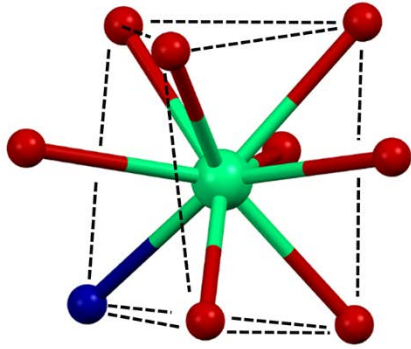


Spectral tuning and emission enhancement through  
lanthanide coordination in a dual Vis-NIR emissive  
cyanide-bridged heterometallic Ru(II)-Er(III) complex

*Dimitrije Mara, Zhiwang Cai, Silvia Bonabello, Stefano Penna, Rik Van Deun, Paola Deplano,  
Luciano Marchiò, Luca Pilia\* and Flavia Artizzu\**

**Supporting Information**



**Figure S1.** Highlight on the coordination environment of the Er atom in **RuEr**.

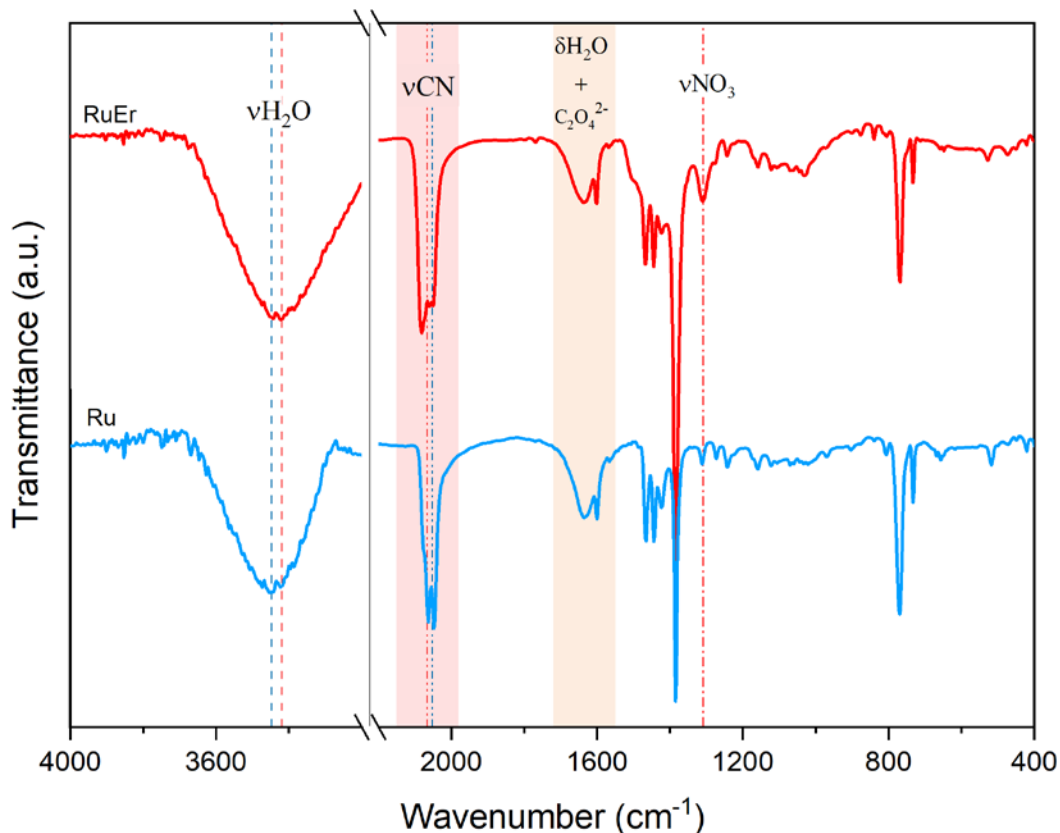


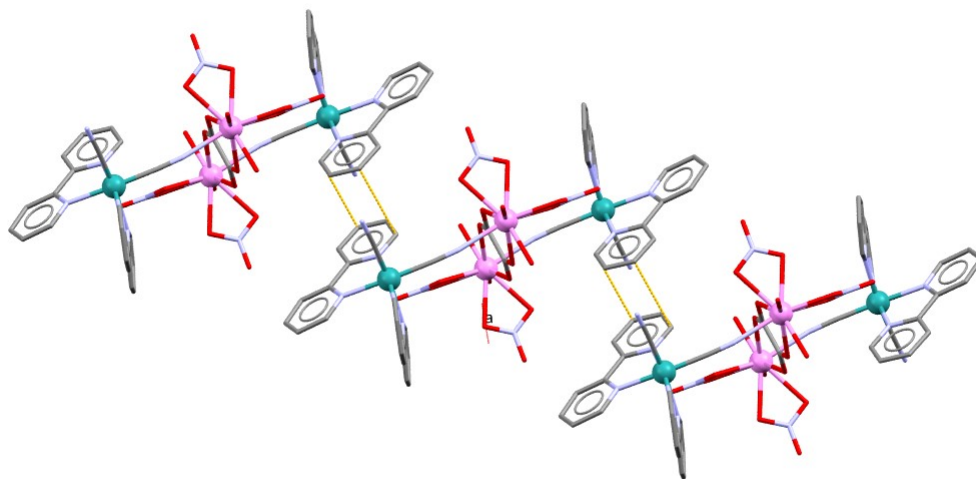
**Figure S2.** FT-IR spectra of **Ru** (in blue) and **RuEr** (in red).

The FT-IR spectra referring to the compounds **RuEr** (in red) and its precursor **Ru** (blue), are both dominated by the peaks attributed to the vibrational modes of the bipy ligand in the region 1550–400  $\text{cm}^{-1}$ . At about 2060  $\text{cm}^{-1}$  a peak related to the stretching mode of the cyanide ion is observed. This peak is slightly shifted towards higher wavenumbers in **RuEr**, likely as a consequence of the coordination to the lanthanide ion. In **RuEr** the peak appears asymmetrically split, a feature that may be related to the presence of one coordinated and one uncoordinated  $\text{CN}^-$  group.

Around 1630  $\text{cm}^{-1}$  a moderately broadened band is observed that is the result of the overlap between the peak related to the bending mode of water molecules and that related to the vibrational mode of oxalate, which is present in both the precursor and the final product. Normalizing the spectra to the peak related to the cyanide ion (and therefore to the  $[\text{Ru}(\text{bipy})_2(\text{CN})_2]$  moiety), it can be seen that the band assigned to oxalate maintains the same intensity in both the precursor and final product. This confirms the presence of the oxalate ion in both the **Ru** and **RuEr** approximately in the same ratio with respect to the  $[\text{Ru}(\text{bipy})_2(\text{CN})_2]$  moiety.

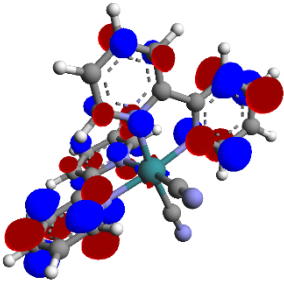
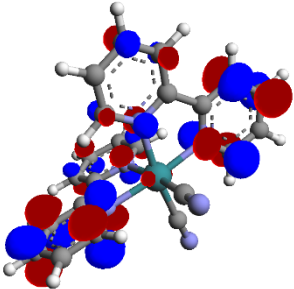
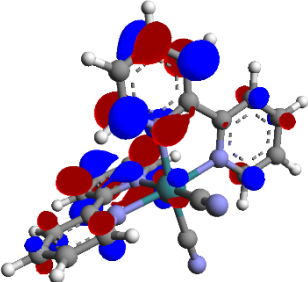
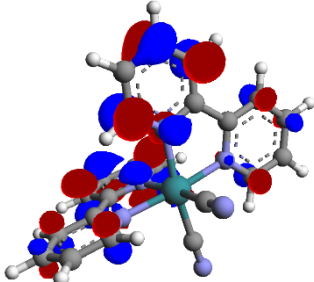
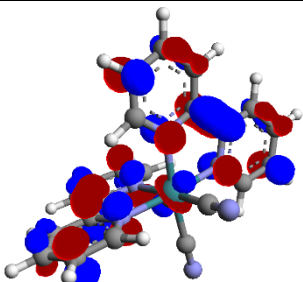
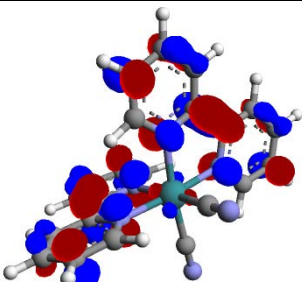
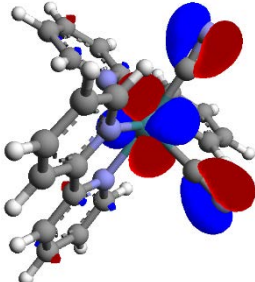
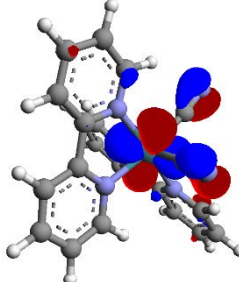
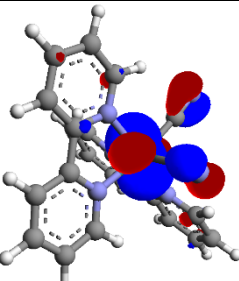
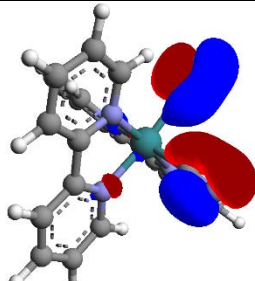
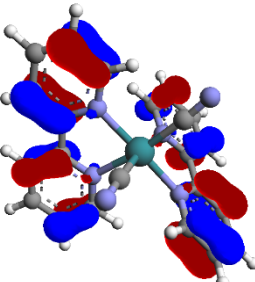
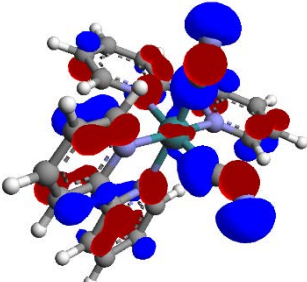
Around 1300  $\text{cm}^{-1}$  a weak peak is identified, probably related to the stretching of the  $\text{NO}_3^-$  group, which is not observed in the precursor.

At around 3400  $\text{cm}^{-1}$ , the broad band related to the symmetric and antisymmetric stretching of water molecules appears slightly shifted to lower wavenumbers in **RuEr** with respect to **Ru**, likely as a consequence of metal coordination and the establishment of strong hydrogen bondings in the crystalline state.



**Figure S3.** Portion of the crystal packing of RuEr highlighting the  $\pi$ -stacking interactions between bipy ligands as dashed yellow lines.

**Table S1.** DFT calculated molecular orbitals of [Ru(bipy)<sub>2</sub>CN<sub>2</sub>] (isovalue plot 0.04) in the gas-phase with corresponding energies (eV).

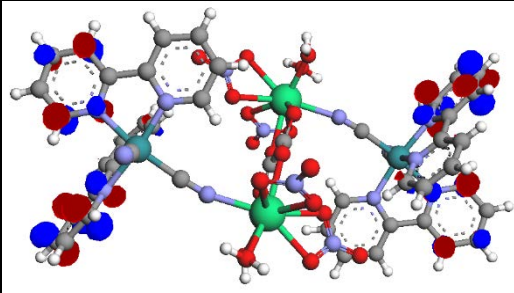
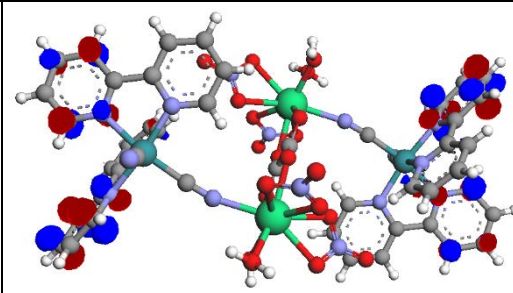
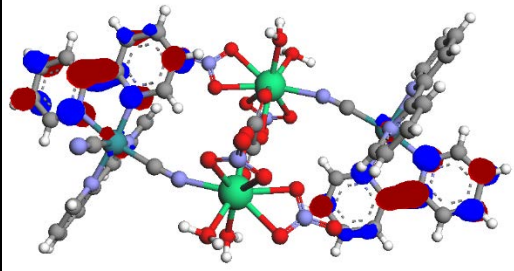
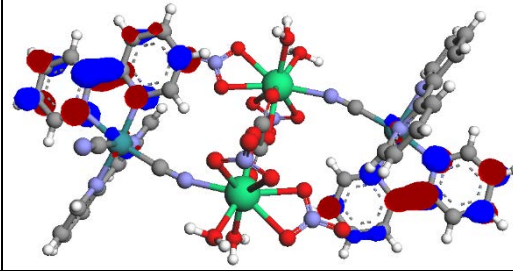
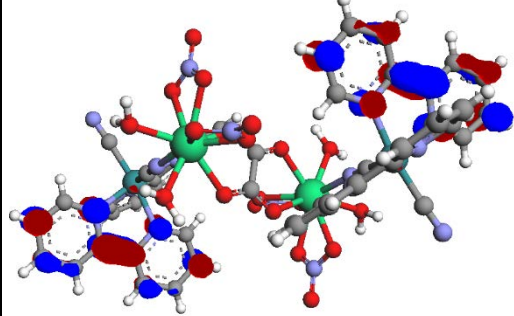
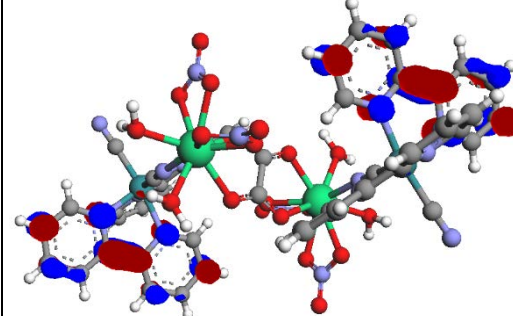
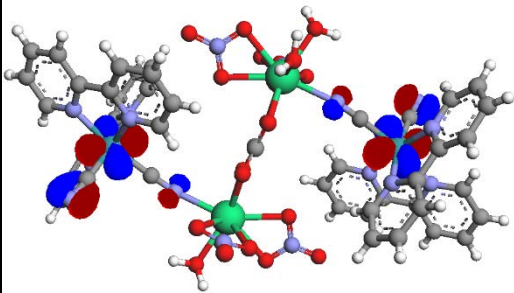
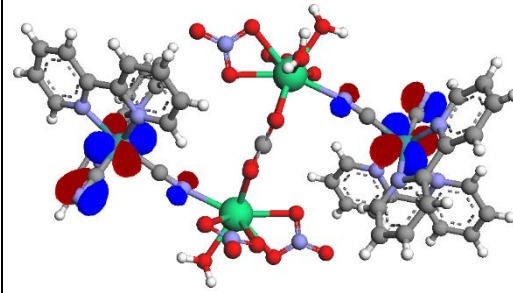
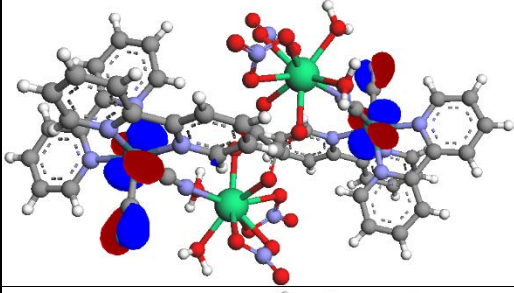
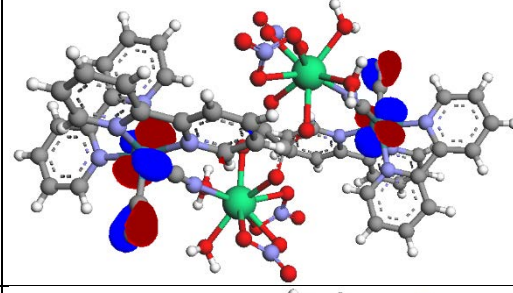
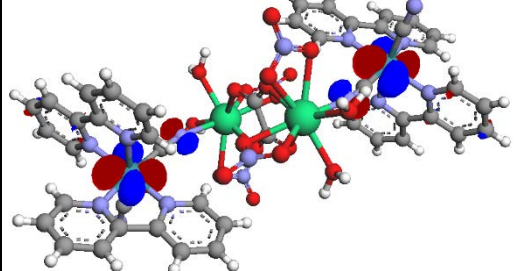
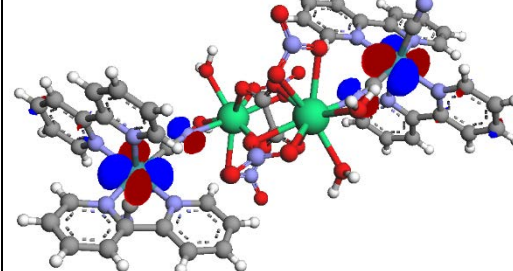
|                  |   |                 |   |
|------------------|---|-----------------|---|
| LUMO+5<br>-0.09  |    | LUMO+4<br>-0.15 |    |
| LUMO+3<br>-0.335 |    | LUMO+2<br>-0.57 |    |
| LUMO+1<br>-1.25  |   | LUMO<br>-1.32   |   |
| HOMO<br>-6.47    |  | HOMO-1<br>-6.73 |  |
| HOMO-2<br>-6.80  |  | HOMO-3<br>-8.34 |  |
| HOMO-4<br>-8.72  |  | HOMO-5<br>-8.73 |  |

**Table S2.** DFT calculated molecular orbitals of [Ru(bipy)<sub>2</sub>CN<sub>2</sub>] (isovalue plot 0.04) in CH<sub>3</sub>CN with corresponding energies (eV).

|                 |  |                 |  |
|-----------------|--|-----------------|--|
| LUMO+5<br>0.05  |  | LUMO+4<br>-0.04 |  |
| LUMO+3<br>-0.16 |  | LUMO+2<br>-0.39 |  |
| LUMO+1<br>-1.15 |  | LUMO<br>-1.21   |  |
| HOMO<br>-7.08   |  | HOMO-1<br>-7.25 |  |
| HOMO-2<br>-7.29 |  | HOMO-3<br>-8.57 |  |
| HOMO-4<br>-8.62 |  | HOMO-5<br>-9.53 |  |



**Table S3.** DFT calculated molecular orbitals of **RuEr** (isovalue plot 0.04) in the gas phase with corresponding energies (eV).

|                 |   |                 |  |
|-----------------|---|-----------------|--|
| LUMO+5<br>-0.52 |    | LUMO+4<br>-0.52 |    |
| LUMO+3<br>-1.01 |    | LUMO+2<br>-1.01 |    |
| LUMO+1<br>-1.29 |   | LUMO<br>-1.29   |   |
| HOMO<br>-6.71   |  | HOMO-1<br>-6.71 |  |
| HOMO-2<br>-6.83 |  | HOMO-3<br>-6.83 |  |
| HOMO-4<br>-7.09 |  | HOMO-5<br>-7.09 |  |

**Table S4.** TD-DFT calculated lowest energy transitions for [Ru(bipy)<sub>2</sub>(CN)<sub>2</sub>] in gas-phase, from optimized structures.

| <b>Calc.<br/>abs. (nm)</b> | <b><math>f^a</math></b> | <b>Major contributions</b>                                       |
|----------------------------|-------------------------|--|
| 436                        | 0.1071                  | H-2->LUMO (85%), H-1->L+1 (7%)                                   |
| 302                        | 0.0586                  | H-1->L+4 (65%), H-1->LUMO+24 (8%), H-1->LUMO+27 (5%)             |
| 259                        | 0.1809                  | H-6->L+1 (15%), H-5->L+1 (17%), H-4->LUMO (37%), H-3->LUMO (13%) |
| 256                        | 0.5617                  | H-6->LUMO (11%), H-5->LUMO (26%), H-4->L+1 (29%), H-3->L+1 (15%) |
| 252                        | 0.0925                  | H-8->LUMO (4%), H-6->LUMO (9%), H-4->L+1 (8%), H-3->L+1 (62%)    |

<sup>a</sup>Calculated oscillator strength; only the transitions with  $f \geq 0.04$  have been reported.



**Table S5.** TD-DFT calculated lowest energy transitions for **RuEr** in the gas-phase.

| Calc.<br>abs. (nm) | $f^a$  | Major contributions  |
|--------------------|--------|--|
| 394                | 0.2248 | H-5(A)->L+1(A) (8%), H-5(A)->L+2(A) (4%), H-4(A)->LUMO(A) (8%), H-4(A)->L+3(A) (4%), H-3(A)->L+1(A) (3%), H-3(A)->L+2(A) (8%), H-2(A)->LUMO(A) (3%), H-2(A)->L+3(A) (8%), H-5(B)->L+1(B) (8%), H-5(B)->L+2(B) (4%), H-4(B)->LUMO(B) (8%), H-4(B)->L+3(B) (4%), H-3(B)->L+1(B) (3%), H-3(B)->L+2(B) (8%), H-2(B)->LUMO(B) (3%), H-2(B)->L+3(B) (8%)   |
| 374                | 0.0350 | H-5(A)->L+2(A) (17%), H-4(A)->L+3(A) (16%), H-5(B)->L+2(B) (17%), H-4(B)->L+3(B) (17%) H-5(A)->L+1(A) (6%), H-4(A)->LUMO(A) (6%), H-5(B)->L+1(B) (6%), H-4(B)->LUMO(B) (6%)  |
| 367                | 0.0986 | H-3(A)->L+2(A) (11%), H-2(A)->L+3(A) (11%), H-3(B)->L+2(B) (11%), H-2(B)->L+3(B) (11%) H-5(A)->L+1(A) (6%), H-4(A)->LUMO(A) (6%), H-1(A)->L+2(A) (3%), HOMO(A)->L+3(A) (3%), H-5(B)->L+1(B) (6%), H-4(B)->LUMO(B) (6%), H-1(B)->L+2(B) (3%), HOMO(B)->L+3(B) (3%)  |
| 327                | 0.0290 | H-1(A)->L+4(A) (21%), HOMO(A)->L+5(A) (21%), H-1(B)->L+4(B) (20%), HOMO(B)->L+5(B) (20%) H-3(A)->L+4(A) (2%), H-2(A)->L+5(A) (2%), H-3(B)->L+4(B) (2%), H-2(B)->L+5(B) (2%)  |
| 319                | 0.0151 | H-3(A)->L+4(A) (21%), H-2(A)->L+5(A) (21%), H-3(B)->L+4(B) (20%), H-2(B)->L+5(B) (20%) H-1(A)->L+4(A) (2%), HOMO(A)->L+5(A) (2%), H-1(B)->L+4(B) (2%), HOMO(B)->L+5(B) (2%)  |
| 309                | 0.0569 | H-1(A)->L+7(A) (19%), HOMO(A)->L+6(A) (19%), H-1(B)->L+7(B) (20%), HOMO(B)->L+6(B) (20%) H-3(A)->L+7(A) (2%), H-2(A)->L+6(A) (2%), H-3(B)->L+7(B) (2%), H-2(B)->L+6(B) (2%)  |
| 302                | 0.0407 | H-5(A)->L+4(A) (15%), H-4(A)->L+5(A) (15%), H-5(B)->L+4(B) (15%), H-4(B)->L+5(B) (15%) H-1(A)->L+8(A) (5%), HOMO(A)->L+9(A) (5%), H-1(B)->L+8(B) (5%), HOMO(B)->L+9(B) (5%)  |
| 295                | 0.0201 | H-5(A)->L+4(A) (3%), H-5(A)->L+7(A) (2%), H-4(A)->L+5(A) (3%), H-4(A)->L+6(A) (2%), H-3(A)->L+7(A) (2%), H-3(A)->L+8(A) (6%), H-3(A)->L+60(A) (2%), H-2(A)->L+6(A) (2%), H-2(A)->L+9(A) (6%), H-2(A)->L+57(A) (3%), H-5(B)->L+4(B) (3%), H-5(B)->L+7(B) (2%), H-4(B)->L+5(B) (3%), H-4(B)->L+6(B) (2%), H-3(B)->L+7(B) (2%), H-3(B)->L+8(B) (5%), H-3(B)->L+66(B) (2%), H-2(B)->L+6(B) (2%), H-2(B)->L+9(B) (5%), H-2(B)->L+63(B) (3%) |
| 290                | 0.0118 | H-5(A)->L+7(A) (11%), H-4(A)->L+6(A) (11%), H-5(B)->L+7(B) (11%), H-4(B)->L+6(B) (12%) H-4(A)->L+57(A) (3%), H-1(A)->L+8(A) (3%), HOMO(A)->L+9(A) (3%), H-4(B)->L+63(B) (3%), H-1(B)->L+8(B) (3%), HOMO(B)->L+9(B) (3%)  |
| 286                | 0.1492 | H-3(A)->L+8(A) (7%), H-3(A)->L+12(A) (2%), H-2(A)->L+9(A) (7%), H-2(A)->L+13(A) (2%), H-1(A)->L+8(A) (6%), HOMO(A)->L+9(A) (6%), H-3(B)->L+8(B) (7%), H-3(B)->L+12(B) (3%), H-2(B)->L+9(B) (7%), H-2(B)->L+13(B) (2%), H-1(B)->L+8(B) (7%), HOMO(B)->L+9(B) (7%)   |

<sup>a</sup>Calculated oscillator strength; only the transitions with  $f \geq 0.01$  have been reported.

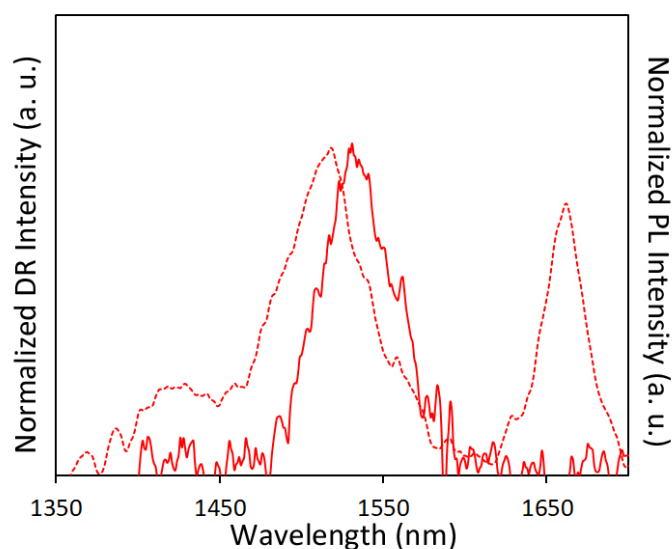


**Figure S4.** Overlaid normalized DR (dashed line) and PL (solid line) spectra of **RuEr** in the NIR.

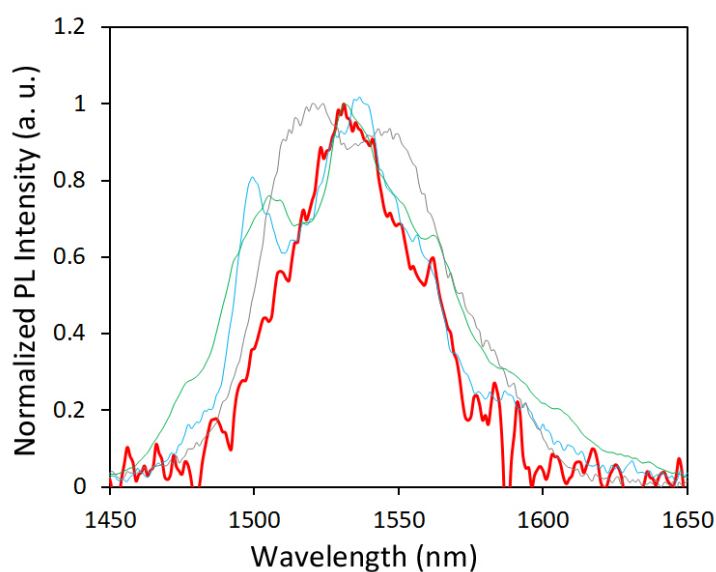


**Figure S5.** Comparison of the Er(III)  $^4I_{13/2} \rightarrow ^4I_{15/2}$  emission spectra normalized to unity of **RuEr** (red thick line)  $\text{Er}_3\text{Q}_9$  (green, Q = 8-quinolinolate),  $[\text{ErCl}(\text{5,7ClQ})_2(\text{H5,7ClQ})_2]$  (blue, H5,7ClQ = 5,7-dichloro-8-hydroxyquinoline) and  $[\text{Er}_2(\text{ClCNA})_3(\text{DMSO})_6]_n$  (grey, ClCNA = chlorocyananilate).

**Table S6.** Integration parameters for the normalized Er(III) emission spectra reported in Figure S5.

| Compound   | Integrated area | FWHM     | Center | Centroid | Ref.      |
|--|-----------------|----------|--------|----------|-----------|
| <b>RuEr</b>  | 58.06728        | 57.25791 | 1531   | 1535.916 | This work |
| $\text{Er}_3\text{Q}_9$                            | 68.69718        | 70.13864 | 1536.5 | 1534.973 | 35        |
| $[\text{ErCl}(\text{5,7ClQ})_2(\text{H5,7ClQ})_2]$ | 76.95706        | 79.06449 | 1531.5 | 1536.218 | 35        |
| $[\text{Er}_2(\text{ClCNA})_3(\text{DMSO})_6]_n$   | 78.26956        | 72.77649 | 1520   | 1537.746 | 36        |